Influence of Cu substitution on structural, morphological and optical properties of Cr/ZnO nanopowders

M. Santhosh[a,*],S. Satheeskumar[a], C.Shanthi[b], B. V. Bhuvaneswari[c]
[a]*Department of Nanoscience and Technology, K S Rangasamy College of Technology, Tiruchengode – 637 215, Tamil Nadu, India*
[b]*Department of Physics, Sona College of Technology, Salem – 636 005, Tamilnadu, India*
[c]*Department of Physics, Alagappa Chettiar Government College of Engineering and Technology, Karaikudi – 630 003, Tamilnadu, India.*

Chromium doped Zinc oxide ($Zn_{0.96}Cr_{0.04}O$), Chromium and Copper co-doped ZnO nanoparticles ($Zn_{0.96}Cr_{0.04}Cu_{0.02}O$ & $Zn_{0.96}Cr_{0.04}Cu_{0.04}O$) successfully synthesized by chemical precipitation method at 500^0C. The crystalline structure, surface morphology and optical properties of the prepared Cr/ZnO and Cr/Cu/ZnO nanoparticles were examined as a function of doping substance and the prepared samples were characterized using XRD, SEM, EDS and UV-Vis spectroscopy analysis. The synthesized nanoparticles show hexagonal wurtzite structure, and the phase segregation takes place for Cu doping. Optical studies revealed that Cr doping increases the energy band gap while Cu incorporation results in decrease of the band gap.

(Received August 20, 2021; Accepted March 2, 2022)

Keywords: Cr/ZnO, Cu/ZnO, Cr/Cu/ZnO, Doping, Co-doping

1. Introduction

Nanotechnology is an important field of existing research dealing with synthesis, strategy, and exploitation of particle's alignment ranging from about 1 to 100nm in size. Within this size range, chemical, physical, and biological properties changed in techniques of both individual atoms/molecules and their consequent size. Novel exploitation of nanoparticles is increasing quickly on diverse fronts due to their totally new or improved properties based on their size and morphology [1,2]. The advancement of the green synthesis procedure for the mixture of nanoparticles is forming into a critical part of nanotechnology [3,4]. The currently synthesized nanomaterial's and their portrayal is a making field of nanotechnology for the earlier two decades, inferable from their vast exploitation in some fields [5].In recent years, lots of researchers have been focused and investigated transition metal oxide nanoparticles [6,7]. The most interest in practical applications of metal oxide nanoparticles such as structural, optical, and magnetic properties. The semiconductors have much interest due to their potential applications when transition metal added as a dopant which includes fuel cells, optical coatings, solid-state lasers, Three-dimensional displays, sensors, platonic devices, etc. [8–10]. Zinc oxide is a wide range bandgap (3.37 eV) semiconducting material which has been widely used in transparent conducting films, gas sensor, and surface acoustic wave device, photocatalyst and optoelectronic devices [11-13]. Unique properties such as low resistivity, non-toxic, highly transparent in the visible range, and high trapping characteristics of ZnO-based materials have been extensively investigated. Recently, many researchers have reported that various morphologies and structures of ZnO can be synthesized by specific synthesis methods. In typical, the functional properties of ZnO nanomaterial can be tailored using physical and chemical methods [14,15]. Moreover, the enhancement of ZnO properties could be further obtained by controlling its structure to be in low dimensional features such as nanowire and nanorods. Metal doped ZnO nanostructures have been

* Corresponding author: msanthosh@ksrct.ac.in
https://doi.org/10.15251/JOR.2022.182.113

of great interest for improving ZnO properties such as electrical, optical, and magnetic to meet the requirement of potential applications. Different physical or chemical methods have been used to prepare ZnO nanoparticles such as thermal decomposition, thermolysis [16], chemical vapor deposition, sol–gel [17], spray pyrolysis, precipitation [18], and co-precipitation [19]. Among these different methods, co-precipitation is one of the most important methods to prepare nanopowder. Co-precipitation is the name given by analytical chemists to a phenomenon whereby the fractional precipitation of a specified ion in a solution results in precipitation not only of target ion but also of other ions existing side by side in the solution. The enhanced ferromagnetic order was observed in Cr and Cu doped ZnO powder where Cu acted as an acceptor [20]. Chakraborti et al. have studied structural and magnetic properties of Zn0.90 Cr0.10O prepared by the co-precipitation technique [21]. He indicated that its inerrant electrons were responsible for the ferromagnetism in Cr, Cu co-doped ZnO. Sato et al. predicted that 3d transition metal atoms of Mn, Fe, Co, and Ni show ferromagnetic ordering in ZnO [22]. Hou et al. observed the transition temperature of Zn0.98 Cu0.02O was to be about 350K but was decreased to 320K with nitrogen doping [23]. The influence of shape and hydrogenation on ferromagnetic properties of Zn0.93 Cr0.05 Cu0.02O nanoparticles at room temperature was demonstrated by Xu et al. [24]. Even though some of the research works have been carried out on Cu and Cr co-doped ZnO system [25,26], most of the works are on the nanoparticles and comprehensive study of the structural and optical properties of Cu and Cr co-doped ZnO nanomaterials is still scanty. According to our literature survey, there is no one study present Cr and Cu co-doped ZnO nanomaterials. Therefore, in the present investigation, Cr doped ZnO and different concentrations of Cr and Cu co-doped ZnO nanomaterials have been synthesized by the co-precipitation method. The effect of Cu substitution on its structural, optical and morphological has been studied extensively. Further, the size-dependent properties of the nanoparticles are correlated with bandgap.

2. Experimental details

2.1. Materials& Methods

The high purity chemicals (499% purity) such as zinc (II) nitrate hexahydrate (Zn (NO3)2 6H2O), copper (II) nitrate tri-hydrate (Cu (NO3)2 3H2O), chromium (II) nitrate hexahydrate (Cr (NO3)2 6H2O) were used as precursors without further purification. Initially, the appropriate amounts of ethanol and water (1:4 ratios) were mixed systematically using a magnetic stirrer. Then the appropriate amounts of zinc nitrate, chromium nitrate, and copper nitrate were dissolved in ethanol solution and kept in a magnetic stirrer for 2h under constant stirring. A separate NaOH solution was prepared by dissolving appropriate amounts of sodium hydroxide in the double-distilled water. The pH value of the solution was selected as 4.6 for a better precipitation reaction. The prepared NaOH solution was then added drop-wise to the initial solution under constant stirring for 2h at room temperature to produce a white, gelatinous precipitate. The white precipitates were filtered and washed with distilled water many times. The final precipitates were dried in the oven at 80^{o}C for 2h. The dried precipitates were collected and ground in an agate mortar. Finally, the collected nanopowder was annealed at 500oC for 2h under air atmosphere followed by furnace cooling. The same procedure is repeated to the remaining samples synthesized with nominal compositions of Cr/Cu/ZnO nanoparticles. Formations of NPs are confirmed by absorption spectrums measured by a Shimadzu UV-1800 spectrophotometer (Japan) over a wavelength range of 300–700 nm. The crystal structure of Cr/ZnO and different composition of Cr/Cu/ZnO nano powders were determined by powder X-ray diffraction. XRD patterns were recorded on a Riga KuC/max-2500 diffractometer using CuKa radiation (l=1.5408˚A) at 30 kV and 100mA from 2y=101 to 801. The topological features and composition of Zn, O, Chromium and Cu were determined by energy dispersive X-ray spectrometer on K and L lines. The surface morphology of Cr/ZnO and different composition of Cr/Cu/ZnO nano powders were studied using a scanning electron microscope (SEM, JEOL JSM 6390).

3. Results and Discussion

3.1. XRD Structural analysis

The XRD pattern of the Cr/ZnO and different composition of Cu/Cr/ZnO nanoparticles are shown in Fig. 1. The pronounced diffraction peaks in the XRD pattern clearly shows the crystalline nature with sharp peaks corresponding to (100), (002), (101), (102), (110), (103), (200), (112) and (201) planes. The indexed XRD patterns shows there is no additional peaks corresponding to any impurity and also confirmed the formation of pure phase zinc oxide with hexagonal wurtzite structure nanoparticles (JCPDS card no. 36-1451) [27] with preferred orientation along (101) plane in all the samples. This indicates that the simultaneous substitution of Cr and Cu cannot disturb the structure of ZnO. No additional peaks (such as Cr, CrO, Cu, CuO, and Cu_2O) were observed in Cr/ZnO and different composition of Cu/Cr/ZnO nanoparticles, which indicates no impurity exist in the samples. The crystallite size of ZnO phase is found to decrease with increase in doping concentration of copper from 1 to 3. It increases from 23 nm to 28 nm for the Cu doped ZnO. Even though, there are no secondary phases detected by XRD analysis, the existence of secondary phases cannot be completely excluded due to limitation of this characterization technique [28]. It is noticed from Fig. 1 that the peak intensity increases with Cu concentration, which means that the crystalline quality is improved with Cu doping and also Cu^{2+} ion is understood to have occupied Zn^{2+} without changing crystal structure. Wei et al., reported the same trend, the increase of diffraction peak intensity with Cu doping [29]. Furthermore, the inset of Fig. 1 clearly shows diffraction peak along (101) plane is shifted towards the lower diffraction angle gradually with addition of Cu concentrations. The small shift of diffraction peak (2θ=0.0331 for un-hydrogenated samples and 2θ=0.0341 for hydrogenated samples) towards the lower angle and increase of peak intensity indicates that Cu^{2+} ions are doped into Zn–Cr–O crystal lattice successfully in the position of Zn^{2+} ions and also the crystal lattice has no obvious change by Cu doping.

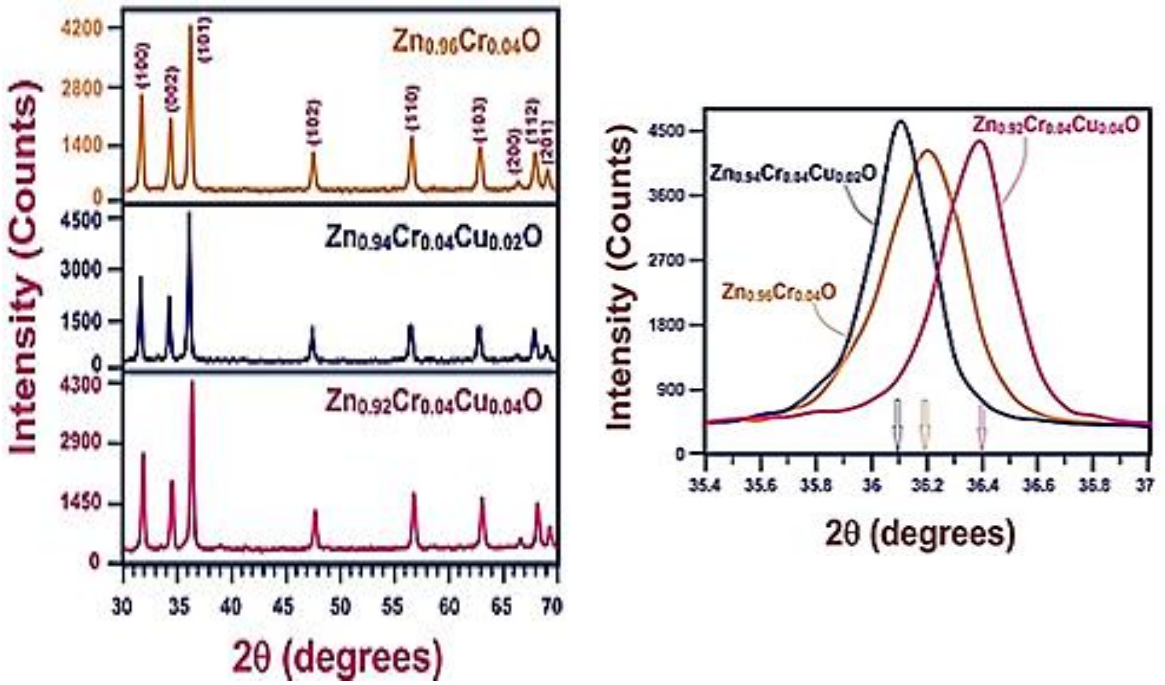

Fig. 1. X-ray diffraction of $Cr_{0.04}Zn_{0.96}O$, $Cr_{0.04}Cu_{0.02}Zn_{0.94}O$ and $Cr_{0.04}Cu_{0.04}Zn_{0.92}O$ Nanoparticles.

3.2. SEManalysis

Figure 2 shows SEM images of the Cr/ZnO and different composition of Cu/Cr/ZnO

nanoparticles. It is observed that synthesized nanoparticles shows multiple shaped morphology with particle size in the range of 23–28 nm with a little aggregation. The average particle size of $Zn_{1-x}Cr_{0.04}Cu_xO$ sample varies between 23.2, 27.8 and 25.6nm for a, b and c samples respectively. The increase of Cu doped concentrations causes more defects and deformed lattice structures. A good correlation is found to exist between mathematical calculations from XRD analysis and the SEM studies. SEM is one of the promising techniques for the topography study of the samples and it gives important information regarding shape and size of the particles. The surface morphology of the Cr/ZnO and different composition of Cu/Cr/ZnO nanoparticles were as shown in Fig. 2 a, b and c, respectively. The SEM micrographs clearly show the average size of nanoparticles is in the order of nanometer size. The SEM images from Fig.2a, b and c clearly show that the particles are uniformly distributed over the surface with good connectivity containing dominant deformed spheroid-like particles. The particle size was slightly increased with Cu concentrations. The average particle size of $Zn_{1-x}Cr_{0.04}Cu_xO$ sample varies between 23.2, 27.8 and 25.6nm for a, b and c samples respectively. The increase of Cu doped concentrations causes more defects and deformed lattice structures. A good correlation is found to exist between mathematical calculations from XRD analysis and the SEM studies.

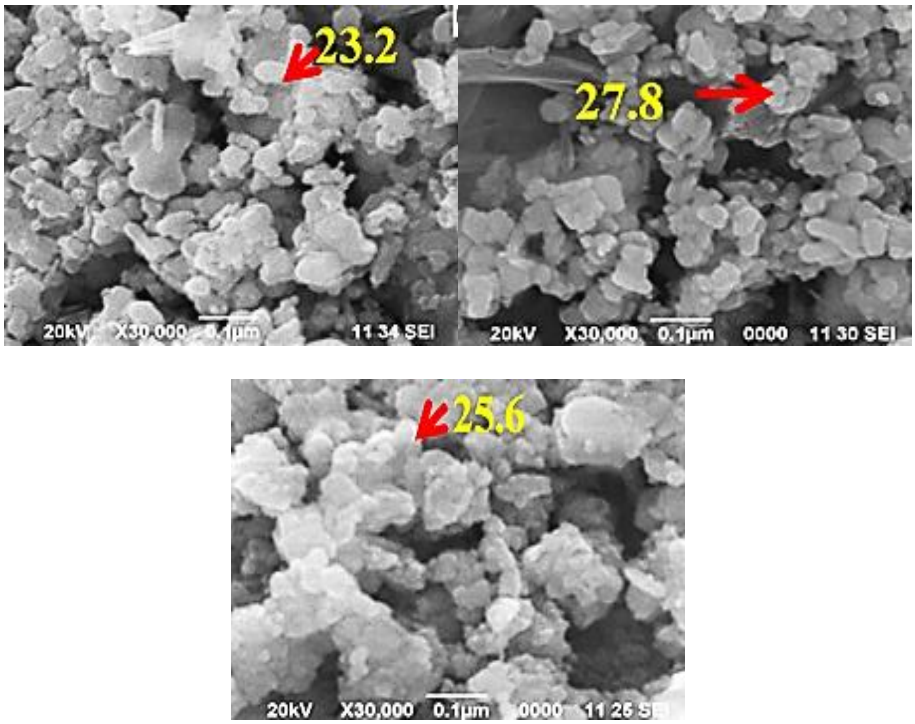

Fig. 2. Scanning electron microscope (SEM) images of a) $Cr_{0.04}Zn_{0.96}O$, b) $Cr_{0.04}Cu_{0.02}Zn_{0.94}O$ andc) $Cr_{0.04}Cu_{0.04}Zn_{0.92}O$ Nanoparticles.

3.3. EDS analysis

The EDS analysis for prepared nanoparticles of Cr/ZnO and different concentration of Cu/Cr/ZnO were analyzed using EDS analysis and the consequences are signified in Figure 3. From the observations, the formation of the Zinc, Oxygen, Chromium and Copper elements of prepared nanoparticles are established. Spectrum of EDS displays no impurities existent in the prepared nanoparticles of $Cr_{0.04}Zn_{0.96}O$, $Cr_{0.04}Cu_{0.02}Zn_{0.94}O$ and $Cr_{0.04}Cu_{0.04}Zn_{0.92}O$. The facts of weight % and atomic % of elements were also established using Spectrum of EDS in Table 1.

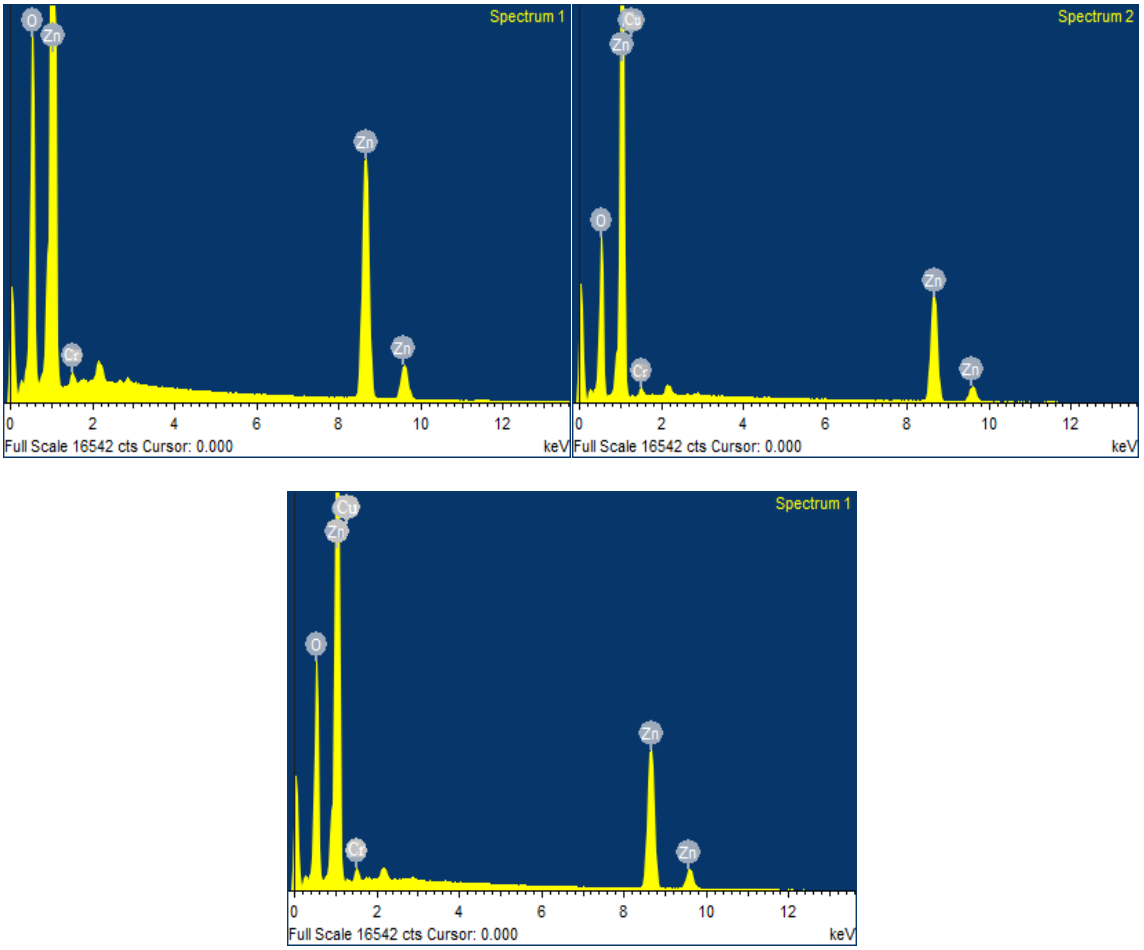

Fig. 3.EADX images of a) $Cr_{0.04}Zn_{0.96}O$, b) $Cr_{0.04}Cu_{0.02}Zn_{0.94}O$ and c) $Cr_{0.04}Cu_{0.04}Zn_{0.92}O$ Nanoparticles.

Table 1. % of Weight for $Cr_{0.04}Zn_{0.96}O$, $Cr_{0.04}Cu_{0.02}Zn_{0.94}O$ and $Cr_{0.04}Cu_{0.04}Zn_{0.92}O$ NPs by EDS Analysis.

NPs	Zinc Weight %	Chromium Weight %	Copper Weight %	Oxygen Weight %
$Cr_{0.04}Zn_{0.96}O$	67.46	3.75	1.02	22.73
$Cr_{0.04}Cu_{0.02}Zn_{0.94}O$	56.33	4.48	1.28	19.37
$Cr_{0.04}Cu_{0.04}Zn_{0.92}O$	52.84	4.32	3.29	15.93

3.4. Optical studies

All the synthesized samples were subjected to UV–Vis spectroscopy at room temperature to observe the band gap of pure and Cr doped ZnO nanoparticles. Figure 4a shows absorption peaks at 340, 341, 344, and 346 nm, for pure, different concentrations of Cr, Cu co-doped ZnO nanoparticles, respectively. Also peaks in all the samples are blue shifted in relationship to bulk ZnO having absorption peak at 375 nm [28]. Using Tauc's plot [20, 24, 29–31], band gap has been obtained which shows relationship between absorption coefficient (a) and incident photon energy (hm) which can be written as ahm ¼ A hmEg n ; where 'A' is constant, 'a' is the absorption coefficient and n depends on transition types. The exact band gap value has been obtained by extrapolating the straight line portion of the $(ahm)^2$ versus hm graph. Figure 4b shows the graphs between $(ahm)^2$ and (hm) for Cr/ZnO and Cr/Cu/ZnO nanoparticles. The band gap values obtained

are 3.49, 3.43, 3.38 and 3.34 eV for $Cr_{0.04}Zn_{0.96}O$, $Cr_{0.04}Cu_{0.02}Zn_{0.94}O$, $Cr_{0.04}Cu_{0.04}Zn_{0.92}O$ and Pure ZnO Nanoparticles, respectively. It has been observed that optical energy band gap of Cr doped ZnO samples are lower than that of pure ZnO and is observed to decrease further with increase in doping concentration. This might be due to the merging of an impurity band into conduction band [32]. UV–Visible absorption spectroscopy is a powerful technique to explore optical properties of semiconducting nanoparticle. The UV–Visible optical absorption spectrum of $Cr_{0.04}Zn_{0.96}O$, $Cr_{0.04}Cu_{0.02}Zn_{0.94}O$, $Cr_{0.04}Cu_{0.04}Zn_{0.92}O$ have been carried out at room temperature using UV–Visible spectrometer (Model: Lambda35, Make: PerkinElmer) from 300 to 700nm. Fig. 4a and b shows the optical absorption spectra of $Cr_{0.04}Zn_{0.96}O$, $Cr_{0.04}Cu_{0.02}Zn_{0.94}O$, $Cr_{0.04}Cu_{0.04}Zn_{0.92}O$ samples, respectively. The absorption spectra show that the absorption of the doped samples was increased with increasing Cu concentrations. The inset of Fig. 4a and b shows the clear picture of absorption changes around 468nm.The absorption edge of $Zn_{1-x}Cr_{0.04}Cu_xO$ sample is found to be 392nm which is shifted towards the higher wavelengths (redshift) with increasing Cu concentrations as b sample has the absorption edge around 398nm; c sample has the edge around 401nm. In the case of hydrogenated samples, the absorption edge is shifted from 396nm (x=0.02) to 403nm (x=0.04) which is slightly higher than the undoped samples. The change in absorption edge in both cases can be attributed to the photo-excitation of electrons from valence band to conduction band. The same red shift by Cu doping was noticed in the literature [31]. The energy band gap of the $Cr_{0.04}Zn_{0.96}O$, $Cr_{0.04,}$ $Cu_{0.02}Zn_{0.94}O$, $Cr_{0.04}Cu_{0.04}Zn_{0.92}O$ can be obtained by plotting $(\alpha hy)^2$ versus $h\gamma$ and extrapolating the linear portion of the absorption edge to find the intercept with energy axis as shown in Fig. 4b. The overall band gap is gradually decreased from 3.72 to 3.57eV when Cu is increased from 0.02 to 0.04 in the $Zn_{1-x}Cr_{0.04}Cu_xO$ system. The noticed slighted shift in the band gap is due to Cu doping and hydrogenation effect in Zn–Cr–O lattice. The similar narrowing of band gap was observed by Diouri et al., in Cu doped ZnO. It is explained by p–d spin-exchange interactions between the band electrons and localized electrons of the transition-metal ion substituting Cu^{2+} ion [32]. The reduction of band gap by Cu doping is also due to strong p–d mixing of O and Cu [33]. This is also in good agreement to the quantum confinement effect of the nanoparticles [34].

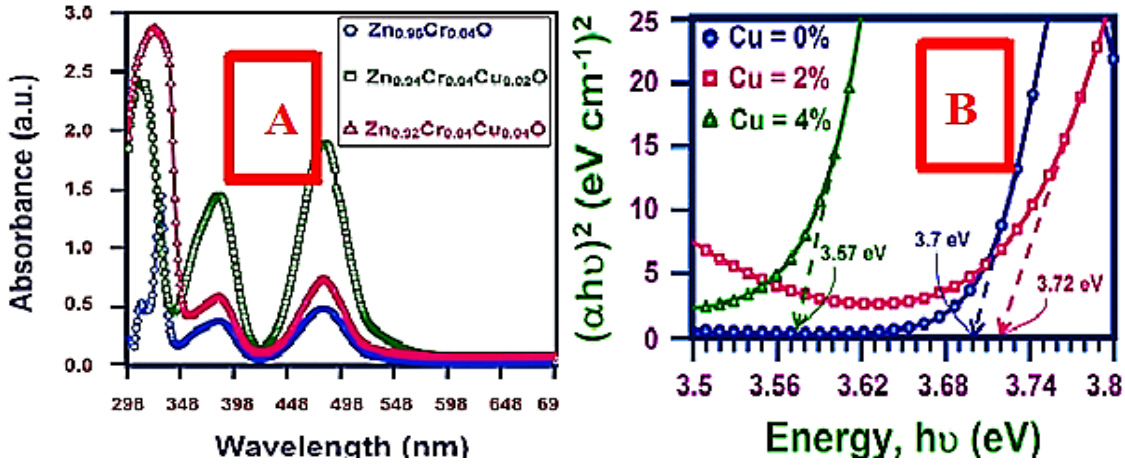

Fig. 4.A) UV-Absorbance spectra and B) Tauc's plot of $Cr_{0.04}Zn_{0.96}O$, $Cr_{0.04}Cu_{0.02}Zn_{0.94}O$ and $Cr_{0.04}Cu_{0.04}Zn_{0.92}O$ Nanoparticles.

4. Conclusions

$Cr_{0.04}Zn_{0.96}O$, $Cr_{0.04}Cu_{0.02}Zn_{0.94}O$, $Cr_{0.04}$and$Cu_{0.04}Zn_{0.92}O$ nanomaterials have been synthesized by co-precipitation method at 500^0C. The XRD and SEM measurements revealed the substitution of Cu in the Zn–O–Cr lattice without changing the hexagonal wurtzite structure. From XRD analysis, nanosize of the prepared nanoparticles increases from 23 nm to 28 nm and from SEM analysis observations, multiple shaped morphology with particle size in the range of 23–28

nm with a little aggregation the pureness of the nanoparticles were confirmed using EDS analysis.

The band gap values obtained tauc's plot and it was 3.49, 3.43 and 3.38 eV for $Cr_{0.04}Zn_{0.96}O$, $Cr_{0.04}Cu_{0.02}Zn_{0.94}O$, $Cr_{0.04}$and$Cu_{0.04}Zn_{0.92}O$ Nanoparticles. It has been observed that optical energy band gap of Cr doped ZnO samples are lower than that of pure ZnO and is observed to decrease further with increase in doping concentrations. The increase of lattice constants, the average particle size, the slight shift of XRD peaks and the reduction in the band gap indicated that Cu had really doped in to the Zn–O–Cr lattice.

References

[1] C. A. Dos Santos, M. M. Seckler, A. P. Ingle, I. Gupta, S. Galdiero, M. Galdiero, A. Gade, M. Rai, J. Pharm. Sci.103, 1931 (2014); https://doi.org/10.1002/jps.24001

[2] K. B. Narayanan, N. Sakthivel, Adv. Colloid Interface Sci. 156,1 (2010); https://doi.org/10.1016/j.cis.2010.02.001

[3] P. Raveendran, J. Fu, S. L. Wallen,Green Chem.8, 34 (2006); https://doi.org/10.1039/B512540E

[4] V. Armendariz, J. L. Gardea-Torresdey, M. Jose Yacaman, J. Gonzalez, I. Herrera, J. G. Parsons, Proceedings of Conference on Application of Waste Remediation Technologies to Agricultural Contamination of Water Resources, (2002).

[5] J. Y. Song, B. S. Kim, Bioprocess,BiosystEng.32, 79 (2008); https://doi.org/10.1007/s00449-008-0224-6

[6] Haja Hameed Abdul RahmanSyedahamed, ChandrasekaranKarthikeyan, SeemaisamySasikumar, VenugopalSenthil Kumar, J. Mater. Chem. B 1, 5950 (2013); https://doi.org/10.1039/c3tb21068e

[7] Jinbo Cao, Junqiao Wu, Mater. Sci. Eng. R Rep. 71,35 (2011).

[8] Jinsub Park, Dong Su Shin, Do-Hyun Kim, J. Alloys Compd. 611, 157 (2014); https://doi.org/10.1016/j.jallcom.2014.05.019

[9] P.V. Rajkumar, K. Ravichandran, M. Baneto, C. Ravidhas, B. Sakthivel, N. Dineshbabu, Mater. Sci. Semicond. Process. 35, 189 (2015); https://doi.org/10.1016/j.mssp.2015.03.010

[10] M. El-Hilo, A.A. Dakhel, J. Magn. Magn Mater. 323, 2202 (2011); https://doi.org/10.1016/j.jmmm.2011.03.031

[11] Y. Ning, Q. Junjie, Zi Qi, XiaomeiZh, YaYa, Jing Li, Yue Zh,J Power Sorces195,5806 (2010).

[12] C. Shalaka, Navale, I. S. Mulla, Materials science and engineering C 29, 1317 (2009); https://doi.org/10.1016/j.msec.2008.09.050

[13] G. N. Manjula, M. Nirmala, K. Rekha, A. Anukaliani, Mater Lett. 65, 1797 (2011); https://doi.org/10.1016/j.matlet.2011.03.079

[14] C. A. Yasemin, A. K. Seval, I. L. Saliha, C. A. Mujdat,SuperlatticeMicrost, 46, 469 (2009).

[15] W. A. Jiaheng, Lei Me, Yang Qi, Maolin Li, GuimeiSh, Meili Li,J Cryst Growth311,2305 (2009).

[16] M.S. Niasari, F. Davar, A. Khansari, J. Alloys Compd. 509, 61 (2011); https://doi.org/10.1016/j.jallcom.2010.08.060

[17] J. Yang, L. Feia, H. Liua, Y. Liu, M. Gao, Y. Zhang, L. Yang, J. Alloys Compd. 509, 3672 (2011); https://doi.org/10.1016/j.jallcom.2010.12.157

[18] Y. Yang, H. Chen, B. Zhao, X. Bao, J. Cryst. Growth 263, 447 (2004); https://doi.org/10.1016/j.jcrysgro.2003.12.010

[19] R. Chauhan, A. Kumar, R.P. Chaudhary., J. Chem. Pharm. Res. 2, 178 (2010).

[20] Y. Wei, D. Hou, S. Qiao, C. Zhen, G. Tang, Physica B404, 2486 (2009); https://doi.org/10.1016/j.physb.2009.05.008

[21] D. Chakraborti, S. Ramachandran, G. Trichy, J. Narayan, J. Appl. Phys. 101, 053918 (2007); https://doi.org/10.1063/1.2711082

[22] K. Sato, H.K. Yoshida, Jpn. J. Appl. Phys. 40, L334 (2001); https://doi.org/10.1143/JJAP.40.L334

[23] D.L. Hou, X.J. Ye, H.J. Meng, H.J. Zhou, X.L. Li, C.M. Zhen, G.D. Tang, Appl. Phys. Lett. 90, 142502 (2007); https://doi.org/10.1063/1.2719034

[24] H. Xu, Q. Zhao, H. Yang, Y. Chen, J. Nanopart. Res. 11, 615 (2009); https://doi.org/10.1007/s11051-008-9444-6

[25] Z. Quan, D. Li, B. Sebo, W. Liu, S. Guo, S. Xu, H. Huang, G. Fang, M. Li, X. Zhao, Appl. Surf. Sci. 256, 3669 (2010); https://doi.org/10.1016/j.apsusc.2010.01.005

[26] H.T. Lin, T.S. Chin, J.C. Shih, S.H. Lin, T.M. Hong, R.T. Huang, F.R. Chen, J.J. Kai, Appl. Phy. Lett. 85,621 (2004); https://doi.org/10.1063/1.1775877

[27] A. Askarinejad, A. Morsali, Ultrason. Sonochem. 16,124 (2009); https://doi.org/10.1016/j.ultsonch.2008.05.015

[28] Y. Wei, D. Hou, S. Qiao, C. Zhen, G. Tang, Physica B 404, 2486 (2009); https://doi.org/10.1016/j.physb.2009.05.008

[29] Jagannatha Reddy, M.K. Kokila, H. Nagabhushan, R.P.S. Chakradhar, C. Shivakumar, J.L. Rao, B.M. Nagabhushan, J. Alloys Compd. 509, 5349-5355(2011); https://doi.org/10.1016/j.jallcom.2011.02.043

[30] K. Park, D.J. Chadi, Phys. Rev. Lett. 94,127204 (2005); https://doi.org/10.1103/PhysRevLett.94.127204

[31] J. Diouri, J.P. Lascaray, M. El Amrani, Phys. Rev. B 31, 7995 (1985); https://doi.org/10.1103/PhysRevB.31.7995

[32] M. Ferhat, A. Zaoui, R. Ahuja, Appl. Phys. Lett. 94, 142502 (2009); https://doi.org/10.1063/1.3112603

[33] T. Takagahara, K. Takeda, Phys. Rev. B 46, 15578 (1992); https://doi.org/10.1103/PhysRevB.46.15578

[34] A. Thill, O. Zeyons, O. Spalla, F. Chauvat, J. Rose, M. Auffan, Environ Sci Technol. 40(19), 6151 (2006); https://doi.org/10.1021/es060999b

[35] J. Wang, H. Liu, T. Kurtan, A. Mandi, A. Sandor, L. Jia, H. Zhang, Y. Guo, Org BiomolChem. 9(22), 7685 (2011); https://doi.org/10.1039/c1ob06150j

[36] C. L. Dupont, G. Grass, C. Rensing, Metallomics3, 1109 (2011); https://doi.org/10.1039/c1mt00107h